Experimental Electrical Characterization of Interconnects and Discontinuities in High-Speed Digital Systems

Steven B. Goldberg, *Member, IEEE,* Michael B. Steer, *Senior Member, IEEE,*
Paul D. Franzon, *Member, IEEE,* and Jeffrey S. Kasten

Abstract—**As clock speeds increase, electrical simulation of interconnects becomes essential in engineering design. In spite of the availability of a variety of electromagnetic modeling tools, experimental characterization is required to verify and, in some cases, to develop models of lines and interconnect discontinuities for use in simulation. In this paper we present measurement techniques to experimentally characterize the electrical performance of interconnects on printed circuit boards (PCB's) and multichip modules (MCM's). Novel techniques are presented for calibrated measurements of two- and three-port structures. Measurements of a transmission line, a via, and a tee on a PCB are presented.**

I. Introduction

PRESENT day high end printed circuit board (PCB) and multichip module (MCM) based digital systems require that transmission line and discontinuity effects be incorporated in transient system simulation. High-speed digital signals have significant frequency components up to RF and microwave frequencies. A signal with a rise time of t_r has significant frequency components up to a frequency $f_{\max} = 0.35N/t_r$ where $N = 5$ for most digital systems. Accurate interconnect simulation, therefore, requires accurate interconnect models up to $f_{\max}$ [1]. Thus signals with a rise time of 1 ns, for example, require models up to at least 1.75 GHz. With the improved packaging obtained with MCM's and advanced VLSI devices, models valid at yet higher frequencies will be required.

The traditional approach to interconnect model development is to fit physically-based analytic models to detailed field theoretic simulations. In the case of transmission lines, quasi-static analysis yields capacitance and inductance per unit length parameters. For discontinuities, quasi-static analysis yields lumped element equivalent circuit models. Using a perturbation assumption, corrections are made for frequency dependent effects such as the skin effect. Extending field theoretic models to handle full three-dimensional structures is not at all straightforward and a major penalty is incurred in terms of simulation time. In any case, experimental verification is required to obtain confidence in the validity of models of interconnect structures.

The measurement requirements for PCB's and MCM's are somewhat relaxed compared to those for microwave circuits; however, typically, many measurements are required to calibrate models, to investigate the characteristics of various nonhomogeneous PCB and MCM technologies, and to investigate statistical variations. MCM and PCB interconnects are dissipative so that the traditional planar circuit calibration techniques (which require lossless line standards) cannot be directly used. The purpose of this paper is to present experimental procedures suited to characterization of microstrip and stripline interconnects and discontinuities on PCB's and MCM's. In particular, techniques are developed for calibrated two- and three-port measurements using novel calibration schemes.

II. Two-Port Calibration

At RF and microwave frequencies, significant measurement errors are introduced by fixturing. In the case of two-port measurements, these errors can be removed by inserting known standards. This can be conveniently done in a coaxial line-based measurement system as precisely known standards are readily available. However, precisely known standards are not available for calibration of a planar measurement system. In the work described here, the measurement system is calibrated in a two-tier process [2] wherein the automatic network analyzer is first calibrated to the end of the coaxial cables using a conventional open short load method. Then, the fixture de-embedding is performed using *in-situ* standards. The use of a separate calibration substrate (as used in [3]) is avoided because of the geometrical and dielectric mismatch between the calibration substrate and the device under test.

The through reflect line (TRL) technique is the preferred method for characterizing the fixtures of a planar measurement system [4], [5]. The primary reason for this is that a matched load is not required in the calibration procedure. Instead a through connection, an arbitrary reflection, and a reference transmission line are used as standards and these are easily modeled and constructed. The arbitrary reflection need not be precisely known as long as it is large and can be repeatably placed at the internal ports of the test fixtures. It is

Manuscript received April 15, 1991; revised July 15, 1991. This work was supported in part by the National Science Foundation under Grant MIPS-9017054 and BNR. This paper was presented at the 41st Electronic Components and Technology Conference, Atlanta, GA, May 13–16, 1991.

S. B. Goldberg, M. B. Steer, and P. D. Franzon are with High Frequency Electronics Laboratory, Department of Electrical and Computer Engineering, North Carolina State University, Raleigh, NC 27695-7911.

J. S. Kasten was with North Carolina State University. He is now with the Federal Systems Division, IBM, Owego, NY 13827.

IEEE Log Number 9103141.

0148-6411/91$01.00 © 1991 IEEE

shown that this standard can be synthesized when the two fixtures are identical, yielding a symmetrical through connection—hence, the term through symmetry line (TSL) calibration. This is combined with an improved enhanced through reflect line (ETRL) calibration scheme [6].

A. Through Symmetry Line (TSL)

Calibration schemes assuming identical fixtures and using just a through and a line as standards have previously been reported [7]–[11]. The techniques require the use of specialized calibration software whereas the present development of this approach enables the method to be used with standard TRL de-embedding software. Close matching of the test fixtures can readily be achieved up to low microwave frequencies and at higher frequencies through careful design. The resulting symmetrical through connection enables the reflection coefficient at the external fixture ports to be calculated when the internal fixture ports are terminated in ideal open or short circuits. Referring to the signal flow graph of Fig. 1, the S parameters of the through connection are ${}^{T}S_{11}(={}^{T}S_{22})$ and ${}^{T}S_{21}(={}^{T}S_{12})$, and the actual S parameters of the A network ${}^{A}S_{11}$, ${}^{A}S_{21}={}^{A}S_{12}$ and ${}^{A}S_{22}$, respectively. In addition, the input reflection coefficient with an ideal short circuit placed at port 2 A of A is

$$\rho_{sc}={}^{A}S_{11}-\frac{{}^{A}S_{21}^{2}}{1+{}^{A}S_{22}}. \quad (1)$$

Using Mason's rule to relate the fixture parameters to the individual network parameters, we have the results

$${}^{T}S_{11}={}^{A}S_{11}+\frac{{}^{A}S_{21}^{2}\,{}^{A}S_{22}}{1-{}^{A}S_{22}^{2}} \quad (2)$$

$${}^{T}S_{21}=\frac{{}^{A}S_{21}^{2}}{1-{}^{A}S_{22}^{2}}. \quad (3)$$

By combining (1)–(3), the short circuit reflection coefficient is

$$\rho_{sc}={}^{T}S_{11}-{}^{T}S_{21}. \quad (4)$$

Similar results are obtained for an ideal open circuit placed at port 2 A:

$$\rho_{oc}={}^{T}S_{11}+{}^{T}S_{21}. \quad (5)$$

Thus it is possible to "insert" ideal open and short circuits within a noninsertable medium.

B. Enhanced Through Symmetry Line (ETSL)

The ETSL calibration procedure developed here is a combination of the ETRL technique [6] and the above TSL procedure. Conventional TRL requires an assumption about the characteristic impedance Z_C of the line standard. Generally, this is determined by independent measurement, such as time-domain reflectometry, and is taken to be frequency independent and lossless. However, these are unreasonable assumptions for microstrip and stripline transmission lines on PCB's and MCM's. Normal operating frequencies are such that the skin effect is not fully developed for typical geometries so that frequency-dependent line inductance as well as frequency-dependent line resistance are significant [12]. In ETRL the frequency-dependent complex characteristic impedance is determined using a free space capacitance calculation [6]. An improvement of this technique was proposed in [13], wherein the per unit capacitance of the transmission line was calculated. Unfortunately, the capacitance of a transmission line in a nonhomogeneous region of unknown constituency cannot be calculated. However, at high frequencies, the internal inductance is negligible and so high frequency measurements can be used to determine the effective permittivity of the line. Thus instead of setting the magnitude of the effective permeability, μ_{eff}, equal to unity—the high frequency approximation (as in [6]), becomes

$$\mu_{eff}(f)=-\frac{\gamma^{2}c^{2}}{\epsilon_{eff}\,\omega^{2}} \quad (6)$$

where ϵ_{eff} is the effective permittivity calculated at high frequencies. Then Z_c in [6] becomes

$$Z_c=-j\frac{\gamma}{\epsilon_{eff}\,\omega C_0}. \quad (7)$$

Here, ETRL modified with this correction was combined with the above TSL technique to obtain the enhanced symmetry line (ETSL) technique.

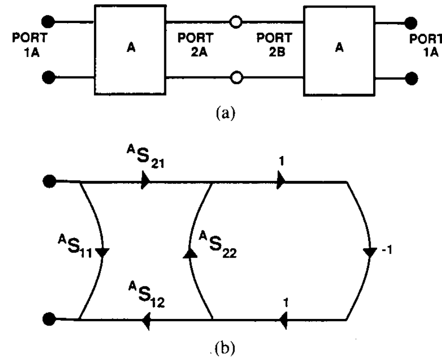

Fig. 1. TSL signal flow graphs. (a) Symmetric fixture diagram. (b) Signal flow graph with ideal short circuit placed at fixture port 1.

III. Two-Port Results

A 3-in microstrip transmission line was tested to determine the error networks of the coaxial-to-microstrip transitions using ETSL. The network analyzer was calibrated to the coaxial reference planes using the network analyzer open short load calibration procedure as the first stage in a two-tier measurement system. A transmission line and a through were connected in turn to the coaxial reference planes and a short circuit reflection coefficient was synthesized. To verify the synthetic reflection standard, a low inductance short circuit was placed at the microstrip reference plane. The short was constructed as a patch with multiple vias to the ground plane. The measured short circuit reflection coefficient is compared in magnitude with the synthesized value in Fig. 2. Agreement

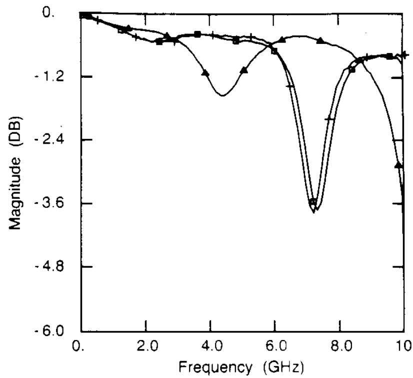

Fig. 2. Magnitude comparison of synthesized and measured short circuit at microstrip reference plane. (+) Measured short circuit reflection coefficient, (□) synthesized, and (△) synthesized open circuit reflection coefficient.

is good and differences can be attributed to the parasitic inductance of the short.

Following establishment of the microstrip reference plane, a 5-in transmission line was characterized and the complex characteristic impedance calculated. Fig. 3 shows the real and imaginary parts of this impedance. Note that the impedance has a $1/\sqrt{f}$ relation as expected [14]. This differs from the results presented in [15] in that the impedance was originally calculated using the method from [6] and a free space capacitance of 31.6 pF/m, calculated analytically, instead of 37.2 pF/m calculated using finite element analysis.

Using the ETSL algorithm, a π equivalent circuit was extracted from the de-embedded S parameters of the PCB via shown in Fig. 4(b). The resulting shunt capacitance and normalized series reactance are shown in Fig. 5. Note that the series reactance behaves as an inductor through 2 GHz and the capacitance is relatively constant to 5 GHz. The increasing capacitance (with frequency) is presumably associated with the increased energy stored in the fringing electric fields and the nonideal inductance arises from resonances with other parasitic capacitances.

IV. Three-Port Calibration

Three-port calibration and characterization of a device must be performed using two-port measurements with the additional port terminated. Traditionally, three-port devices are de-embedded from the test fixture using Wood's renormalization technique [16] or similar iterative techniques [17], [18]. This method, however, becomes inaccurate when a real impedance is not presented to the device's third port. In our approach, two sets of terminations are used to obtain near optimum de-embedding. The relationship between the S parameters of the three-port, S_{ij}, the measured two-port S parameters, S_{ij}^M, and the reflection coefficient presented to the terminated port, Γ_k, is found by using Mason's nontouching loop theorem applied to the signal flowgraph representation of the terminated three-port (Fig. 6). The equation for the two-port reflection S parameter at the ith node is

$$^{mk}S_{ii}^M = S_{ii} + \frac{S_{ki}\,{}^m\Gamma_k S_{ik}}{1 - S_{kk}\,{}^m\Gamma_k} \tag{8}$$

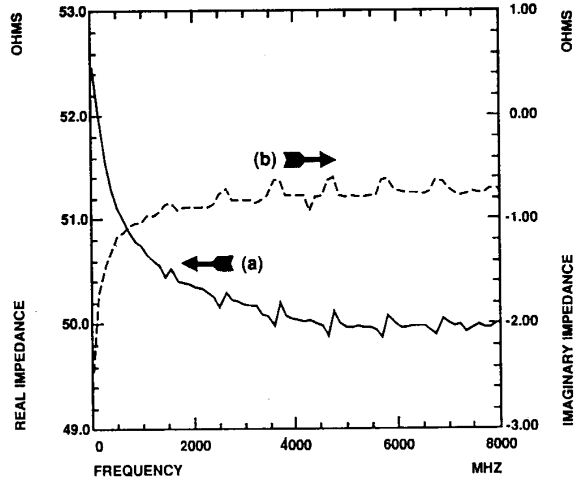

Fig. 3. Characteristic impedance real (solid) and imaginary (dashed) parts of a 5-in transmission line.

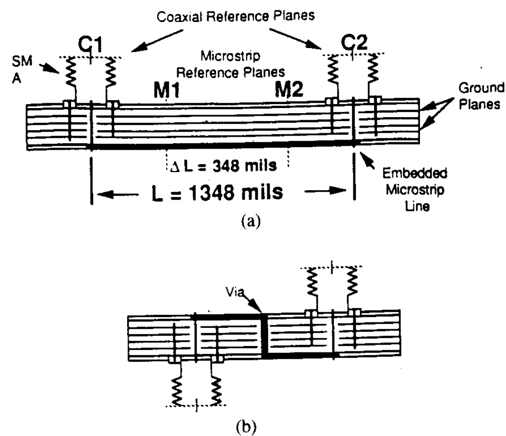

Fig. 4. Diagram of the fixture with line standard inserted (a) and via (b).

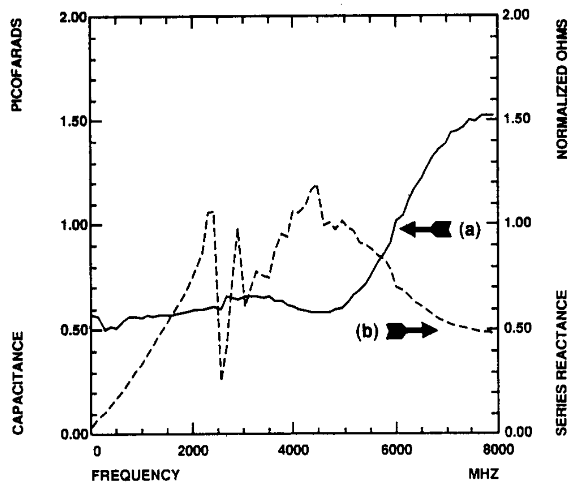

Fig. 5. Via parameters. (a) Shunt capacitance (solid). (b) Series reactance normalized to 50 Ω (dashed).

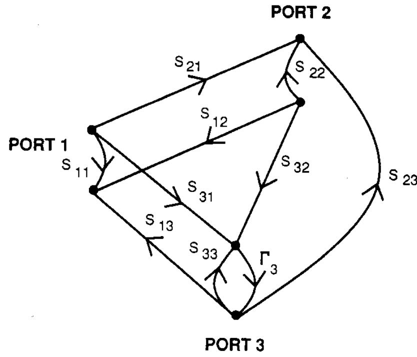

Fig. 6. Signal flow graph of a three-port device with port 3 terminated by reflection coefficient, Γ.

and for transmission

$$^{mk}S_{ij}^M = S_{ij} + \frac{S_{kj}\,{}^m\Gamma_k S_{ik}}{1 - S_{kk}\,{}^m\Gamma_k}. \tag{9}$$

Here, m and k are indexes distinguishing different terminations $^m\Gamma_k$ at port k. The above equations describe 3 sets of two-port S parameter measurements with $i, j, k = 1, 2, 3$; $i \neq j \neq k$. This leads to 12 coupled nonlinear equations which have multiple solutions. The equations can also be poorly conditioned as the measured two-port S parameters are determined to limited accuracy.

In general, good accuracy is obtained when $S_{ii}(S_{ij})$ is evaluated solely in terms of $S_{ii}^M(S_{ij}^M)$ measurements as, usually, they are of the same order. This requires that two different reflection standards be used at each port (so that $m = 1, 2$) and that two-port S parameter measurements be taken for all two-port combinations (that is $i, j, k = 1, 2, 3$, $i \neq j \neq k$). This leads to 24 equations [19] which can be solved as a linear set of equations so that:

$$S_{ii} = \frac{{}^1\Gamma_k{}^2\Gamma_k\left({}^{2k}S_{ii}^M - {}^{1k}S_{ii}^M\right)\left({}^1\Gamma_i^2{}^{2i}S_{kk}^M - {}^2\Gamma_i{}^{1i}S_{kk}^M\right) - \left({}^1\Gamma_i - {}^2\Gamma_i\right)\left({}^1\Gamma_k{}^{2k}S_{ii}^M - {}^2\Gamma_k{}^{1k}S_{ii}^M\right)}{{}^1\Gamma_k{}^2\Gamma_k\left({}^{2k}S_{ii}^M - {}^{1k}S_{ii}^M\right){}^1\Gamma_i{}^2\Gamma_i\left({}^{2i}S_{kk}^M - {}^{1i}S_{kk}^M\right) - \left({}^1\Gamma_i - {}^2\Gamma_i\right)\left({}^1\Gamma_k - {}^2\Gamma_k\right)} \tag{10}$$

and

$$S_{ij} = \frac{\left({}^1\Gamma_k{}^{2k}S_{ij}^M - {}^2\Gamma_k{}^{1k}S_{ij}^M\right) - S_{kk}{}^1\Gamma_k{}^2\Gamma_k\left({}^{2k}S_{ij}^M - {}^{1k}S_{ij}^M\right)}{{}^1\Gamma_k - {}^2\Gamma_k} \tag{11}$$

where S_{kk} is found from (10).

V. Three-Port Results

Multiple two-port measurements of the microstrip tee in the configuration of Fig. 7 were made with the unused port terminated in first, a nominal 50 Ω, and then a short. A total of 6 two-port measurements are required, recognizing the reciprocity of the circuit in this case.

Fig. 8 is a portion of the results that characterize the microstrip tee in the configuration of Fig. 7. As expected, the low frequency reflection and transmission parameters are around 0.33 and 0.67, respectively. Note that the match between S_{11} and S_{33} decreases with frequency, probably due to the increased coupling of the base arm with the two cross arms. De-embedded results obtained using Wood's renormalization technique are reported in [19] and dramatic improvement is seen.

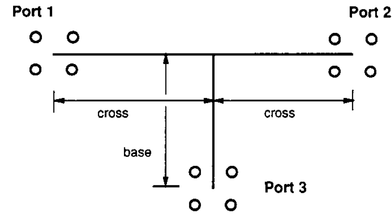

Fig. 7. Configuration of a microstrip tee with arms on the same plane of a PCB.

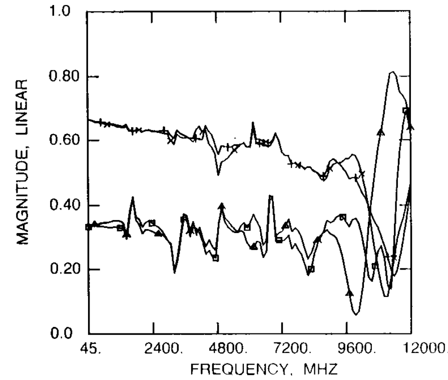

Fig. 8. De-embedded microstrip tee S parameters. Magnitude of (□) S_{11}, (△) S_{33}, (+) S_{31}, and (×) S_{32}.

VI. Discussion and Conclusion

Three measurement techniques suitable for two-port and three-port measurements of interconnects on printed circuit boards and multichip modules were introduced. The techniques achieve calibration using *in-situ* measurements. The first of these, TSL, utilized symmetry to circumvent the problem of inserting reproducible reflection standards. Calibration is achieved using just two standards—a through and a line—thus reducing the substrate area required for calibration. The practicality of this method was shown by comparing the raw reflection coefficient of the synthesized short circuit with those of a fabricated short circuit.

In the second technique, ETRL, the complex impedance of a line standard was determined. This eliminates the impedance error incurred in using the conventional TRL calibration procedure [18]. The procedure was used to de-embed the π equivalent circuit of a PCB via.

A closed-form algorithm that accurately characterizes a three-port device was introduced as the third technique. The technique uses redundant measurements so that three-port reflection parameters are obtained solely in terms of two-port

reflection parameters while transmission parameters are obtained largely in terms of two-port transmission parameters. This procedure dramatically improves the numerical conditioning in determining three-port parameters. Measurements of a three-way tee were reported to demonstrate the robustness of the technique.

The three techniques facilitate rapid measurements of a large number of two-port and three-port interconnects and discontinuities on PCB's and MCM's.

References

[1] L. L. Moresco, "Electronic system packaging: The search for manufacturing the optimum in a sea of constraints," *IEEE Trans. Comp., Hybrids, Manuf. Technol.*, vol. 13, pp. 494-508, Sept. 1990.

[2] R. Vaitkus and D. Scheitlin, "A two-tier de-embedding technique for packaged transistors," in *IEEE MTT-S Int. Microwave Symp. Dig.*, 1982, pp. 328-330.

[3] K. Kiziloglu, N. Dagli, G. L. Matthaei, and S. I. Long, "Experimental analysis of transmission line parameters in high-speed GaAs digital circuit interconnects," *IEEE Trans. Microwave Theory Tech.*, vol. 39, Aug. 1991.

[4] G. F. Engen and C. A. Hoer, "Thru-reflect-line: An improved technique for calibrating the dual six-port automatic network analyzer," *IEEE Trans. Microwave Theory Tech.*, vol. MTT-27, Dec. 1979, pp. 987-993.

[5] C. A. Hoer and G. F. Engen, "Calibrating a dual six-port or four-port for measuring two-ports with any connectors," in *IEEE MTT-S Int. Microwave Symp. Dig.*, 1986, pp. 665-668.

[6] J. S. Kasten, M. B. Steer, and R. Pomerleau, "Enhanced through-reflect-line characterization of two-port measuring systems using free-space capacitance calculation," *IEEE Trans. Microwave Theory Tech.*, vol. 38, pp. 215-217, Feb. 1990.

[7] R. Soares, P. Gouzien, P. Legaud, and G. Follot, "A unified mathematical approach to two-port calibration techniques and some applications," *IEEE Trans. Microwave Theory Tech.*, vol. 37, pp. 1669-1673, Nov. 1989.

[8] K. Silvenon, "Calibration of test fixtures using at least two standards," *IEEE Trans. Microwave Theory Tech.*, vol. 39, pp. 624-629, Apr. 1991.

[9] E. R. Ehlers, "Symmetric test fixture calibration," *IEEE Trans. Microwave Theory Tech.*, vol. MTT-37, pp. 275-278, 1986.

[10] "Measurement and modeling of GaAs FET chips," AVANTEK Application Note, Avantek, Inc., Santa Clara, CA, Oct. 1983.

[11] K. J. Silvonen, "Calibration of test fixtures using at least two standards," *IEEE Trans. Microwave Theory Tech.*, vol. 39, pp. 624-630, Apr. 1991.

[12] G. L. Matthaei, K. Kiziloglu, N. Dagli, and S. I. Long, "The nature of the charges, currents, and fields in and about conductors having cross-sectional dimensions of the order of a skin depth," *IEEE Trans. Microwave Theory Tech.*, vol. 38, pp. 1031-1036, Aug. 1990.

[13] R. B. Marks and D. F. Williams, "Characteristic impedance determination using propagation constant measurements," *IEEE Microwave Guided Wave Lett.*, vol. 1, pp. 141-143, June 1991.

[14] K. Kiziloglu, N. Dagli, G. Matthaei, and S. Long, "Experimental determination of high-speed GaAs digital interconnect parameters," in *IEEE MTT-S Int. Microwave Symp. Dig.*, 1991, pp. 639-642.

[15] S. B. Goldberg, M. B. Steer, P. D. Franzon, and J. S. Kasten, "Experimental electrical characterization of high speed interconnects," in *41st Electronic Components and Technology Conf. Dig.*, May 1991, pp. 85-88.

[16] D. Woods, "Multiport-network analysis by matrix renormalization employing voltage-wave *S*-parameters with complex normalization," *Proc. Inst. Elec. Eng.*, vol. 124, pp. 198-204, Mar. 1977.

[17] M. L. Gabitass, R. K. Froelich, and D. E. Peck, "Automated three-port *s*-parameter measurements," *Microwave J.*, pp. 133-154, 1990.

[18] J. C. Rautio, "A de-embedding algorithm for electromagnetics," *IEEE Int. J. Microwave and Millimeter-Wave Computer-Aided Engineering*, vol. 1, pp. 282-287, 1991.

[19] S. B. Goldberg, M. B. Steer, and P. D. Franzon, "Accurate experimental characterization of three-ports," in *1991 IEEE MTT-S Int. Microwave Symp. Dig.*, June 1991, pp. 241-244.